

# The Subsurface Crack Under Conditions of Slip and Stick Caused by a Surface Normal Force

F.-K. Chang

Maria Comninou

Mem. ASME

Sheri Sheppard

Student Mem. ASME

J. R. Barber

Department of Mechanical Engineering  
and Applied Mechanics,  
University of Michigan,  
Ann Arbor, Mich. 48109

*A solution is given for the elastic stress field in a half plane containing a plane crack parallel to the surface and subjected to a uniform normal pressure and a concentrated normal load. Frictional slip according to Coulomb's law is permitted between the crack faces. As the load is increased, a slip zone originates and grows either from a crack tip or from an intermediate point. Various arrangements of slip and stick zones can occur depending on the magnitude of the load and its location relative to the crack. At very high loads, the crack faces start to separate, but this case is not treated in the present paper.*

## Introduction

The phenomenon of surface slip due to static and moving surface loads has been studied in a series of publications [1-5], which considered the problem of an elastic layer pressed on an elastic substrate. This geometry approximates the contact problem for cylinders with shrink fitted tires. In particular, the results of [5] can be compared with experimental data obtained by Anscombe and Johnson [6] on the rolling of two steel cylinders, one of which is fitted with a steel tire.

A related problem of interest concerns the propagation of a crack parallel to the surface of a solid due to a series of moving loads. Railway wheels, rails, and other surfaces loaded in rolling contact are prone to "spalling failure" in which a subsurface crack propagates parallel to the surface until eventually a thin plate of material is detached, Hundy [7]. The propagation process depends on the stress intensity factors at the crack tips and these will be in turn influenced by frictional contact between the crack faces during the loading cycle as a moving load passes overhead.

In this paper we consider the static situation as a preliminary study to the inherently transient problem of the moving load. When the load is sufficiently high, we find that slip occurs between the crack faces in either one or two zones whose location depends on the position of the load and the extent of the crack. If the slip zones extend to one or both of

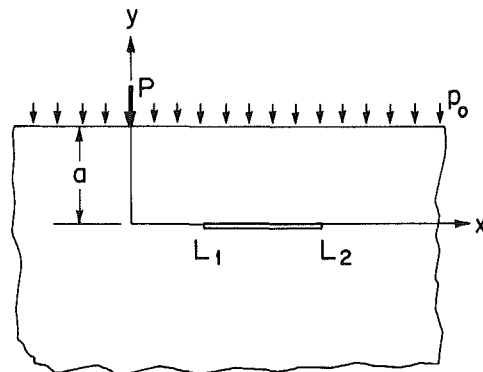


Fig. 1 Geometry of the problem

the crack tips, singular shear tractions are developed ahead of the tip giving a mode II stress intensity factor. Otherwise, the stress field near the tips remains bounded and the frictional contact between the faces inhibits crack propagation. Unfortunately, there are as yet no experimental data with which these results can be compared.

## Formulation

Consider the geometry of Fig. 1. A crack of length  $L_2 - L_1$  is located at depth  $a$  parallel to the surface of an elastic half plane. A compressive force  $P$  and a uniform pressure  $p_0$  are applied on the surface of the half plane. In this analysis, the coordinate system is defined so that the force  $P$  acts at the point  $(0, a)$ , while the location and extent of the crack are considered variable, i.e., the parameters  $L_1, L_2$  may take any (including negative) values. The force is allowed to increase monotonically in magnitude. The faces of the crack can transmit frictional forces and Coulomb's law of friction is assumed.

As long as the crack faces remain in conditions of stick, the

Contributed by the Applied Mechanics Division for presentation at the 1984, PVP Conference and Exhibition, Joint with Applied Mechanics Division and Materials Division, San Antonio, Texas, June 17-21, 1984 of THE AMERICAN SOCIETY OF MECHANICAL ENGINEERS.

Discussion on this paper should be addressed to the Editorial Department, ASME, United Engineering Center, 345 East 47th, Street New York, N.Y. 10017, and will be accepted until two months after final publication of the paper itself in the JOURNAL OF APPLIED MECHANICS. Manuscript received by ASME Applied Mechanics Division, April, 1983; final revision August, 1983. Paper No. 84-APM-17.

Copies will be available until February, 1985.

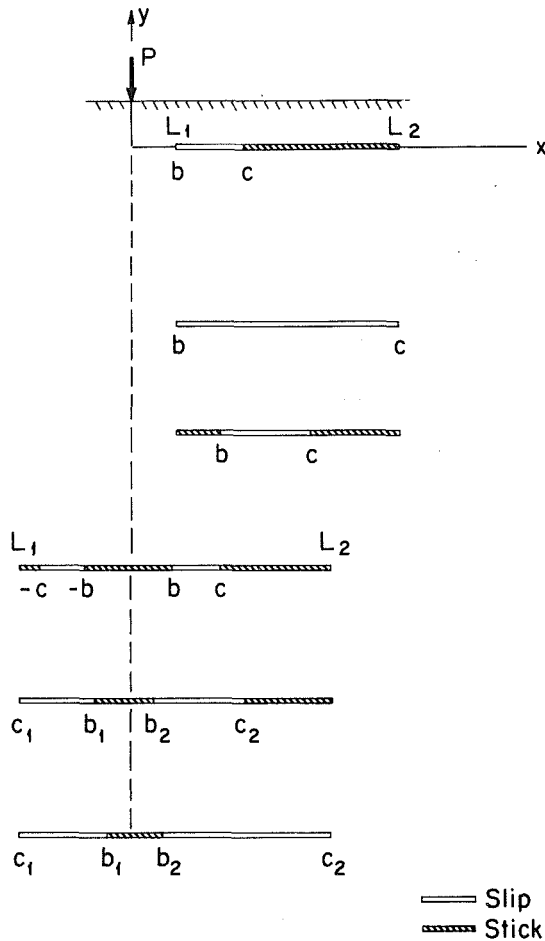


Fig. 2 Arrangements of slip zones (mirror images not shown)

Flamant solution [8] is valid and the tractions on the plane of the crack are

$$\sigma_{xy}(x,0) = \frac{2P}{\pi} \frac{a^2 x}{(a^2 + x^2)^2} \quad (1)$$

$$\sigma_{yy}(x,0) = -p_0 - \frac{2P}{\pi} \frac{a^3}{(a^2 + x^2)^2} \quad (2)$$

The limiting case of a crack extending from  $-\infty$  to  $+\infty$  is the problem of the layer pressed on a substrate treated in [1]. In this case, slip starts at the two symmetric locations  $x^*$  and  $-x^*$  where

$$\left| \frac{x^*}{a} \right| = \frac{1}{3} [(3 + 4f^2)^{1/2} + 2f] \quad (3)$$

when the load  $P$  reaches the critical value  $P^*$  given by

$$\frac{P^*}{p_0 a} = \frac{8\pi f [(3 + 4f^2)^{1/2} + 3 + 2f^2]^2}{27[(3 + 4f^2)^{1/2} - f]} \quad (4)$$

where  $f$  is the coefficient of friction. As the force is increased, the two symmetric slip zones expand in both directions. The ends of the slip zones furthest from the load expand faster than the near ends. The extent and location of the slip zones versus the dimensionless load parameter  $P/p_0 a$  is given in Fig. 6 of [1] for various coefficients of friction. This problem can be used for guidance in the various slip configurations associated with localized slip of the finite extent crack.

Depending on the location of the point  $|x^*|$  in relation to the finite crack we may distinguish the following cases:

I.  $-x^* < x^* < L_1$

II.  $-x^* < L_1 < x^* < L_2$

(a) III.  $L_1 < -x^* < x^* < L_2$

There are three more cases symmetric to the foregoing, which correspond to mirror image slip configurations and are not considered separately.

**Case I.** As the load is increased from  $P^*$ , slip starts for some value  $P > P^*$  at  $L_1$ , leading to the arrangement of Fig. 2(a), where slip occurs in the interval  $b < x < c$ , where  $b = L_1$ . As the load is increased further, the slip zone is expected to expand until it reaches the end point  $L_2$ . The entire crack is then under condition of slip, Fig. 2(b).

(b)

(c)

(d)

(e)

(f)

**Case II.** A slip zone detached from the crack tips appears first in the vicinity of  $x^*$ , Fig. 2(c). As the load increases, the slip zone spreads and it eventually reaches the left or right tip depending on the relative location of  $x^*$ . The arrangement of Fig. 2(a) or its mirror image results. It is also possible to arrive at configuration Fig. 2(e) if  $L_1 < 0$ .

**Case III.** When both points  $|x^*|$  are inside the crack extent and  $L_1 < 0$ , two detached slip zones appear, symmetric about the origin, as shown in Fig. 2(d). As long as slip does not reach the crack tips, their location is immaterial and the situation is identical to that described in [1]. For a finite crack, slip will eventually reach one of the crack tips first, depending on the location of the points  $|x^*|$ . We then have the arrangement of Fig. 2(e) or its mirror image. As the load is further increased, slip penetrates the other crack tip, too, Fig. 2(f).

The analysis follows closely that of [1-3] and only the main steps will be presented here for easy reference. The tractions on  $y = 0$  can be expressed as a sum of two terms. The first term is due to the surface load (Flamant solution and uniform compression) and the second is a corrective solution, the purpose of which is to account for the slip zone(s). The corrective solution is obtained as a distribution of edge dislocations of the glide type with density  $B(x)$ . The possibility of separation (which would require a distribution of climb edge dislocations) is not included in the present formulation. Accordingly, the normal  $N(x)$  and shear  $S(x)$  tractions become

$$N(x) = -p_0 - \frac{2P}{\pi} \frac{a^3}{(a^2 + x^2)^2} + \frac{2\mu}{\pi(\kappa + 1)} \int_{\Gamma} B(\xi) K_n(x, \xi) d\xi \quad (5)$$

$$S(x) = \frac{2P}{\pi} \frac{a^2 x}{(a^2 + x^2)^2} + \frac{2\mu}{\pi(\kappa + 1)} \int_{\Gamma} B(\xi) K_s(x, \xi) d\xi \quad (6)$$

where

$$K_n(x, \xi) = \frac{8a^3}{R^4} \left( -3 + 16 \frac{a^2}{R^2} \right) \quad (7)$$

$$K_s(x, \xi) = \frac{1}{x - \xi} + \frac{x - \xi}{R^2} \left( -1 + \frac{12a^2}{R^2} - \frac{64a^4}{R^4} \right) \quad (8)$$

$$R^2 = 4a^2 + (x - \xi)^2 \quad (9)$$

$\mu$  is the shear modulus and  $\kappa = 3 - 4\nu$  for plane strain,  $\nu$  being the Poisson's ratio. The range of integration  $\Gamma$  is the union of the slip zones (interval  $(b, c)$  or  $(b_2, c_2)$  and  $(c_1, b_1)$ ).

Guided by the Flamant solution, we anticipate positive slip for  $x > 0$  and negative slip for  $x < 0$ . We can then express Coulomb's law in the slip zones(s) as

$$S(x) = -f \operatorname{sgn} x N(x) \quad \text{in } \Gamma \quad (10)$$

$$N(x) \leq 0 \quad \text{in } \Gamma \quad (11)$$

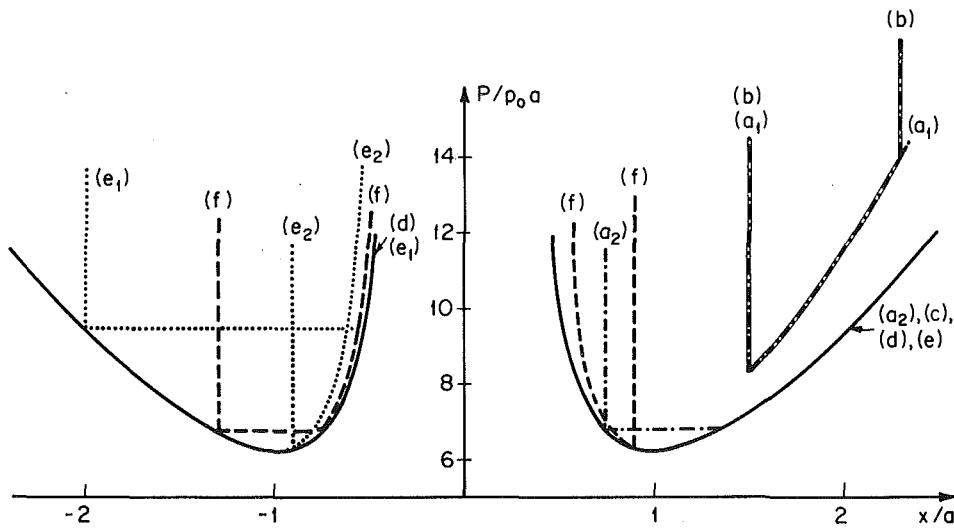


Fig. 3 Dimensionless load versus slip zone location for the arrangements of Fig. 2

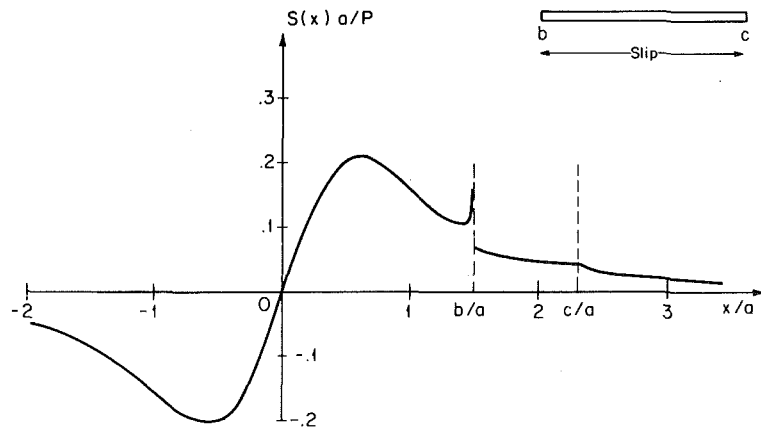


Fig. 4 Shear tractions for arrangement (b) with  $b/a = 1.5$ ,  $c/a = 2.3$ ,  $\lambda = 13.98$

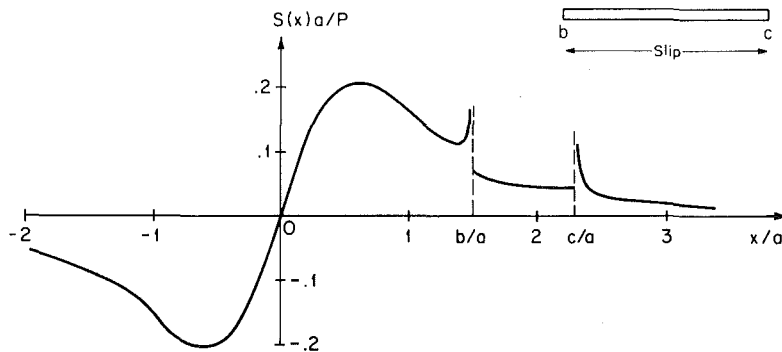


Fig. 5 Shear tractions for arrangement (b) with  $b/a = 1.5$ ,  $c/a = 2.3$ ,  $\lambda = 15$

where  $f$  is the coefficient of friction. For each slip zone we must require that there is no net dislocation left behind or

$$\int_{\Gamma_i} B_x(\xi) d\xi = 0, \quad i = 1, 2 \quad (12)$$

We must also verify that [1]

$$\text{sgn } S(x) = \text{sgn } h(x) \quad (13)$$

where  $h(x)$  is the tangential shift defined as the difference in the tangential displacements on the surfaces  $y = 0^+$  and  $y = 0^-$ . It is also noted that

$$\frac{dh}{dx} = -B(x) \quad (14)$$

In the stick zones that may develop along the crack, we require

$$N(x) \leq 0 \quad (15)$$

$$|S(x)| < -fN(x) \quad (16)$$

Asymptotic analysis has established the behavior of  $B(x)$  at the end points, which is consistent with the boundary conditions of the problem including the inequalities [9]. Thus

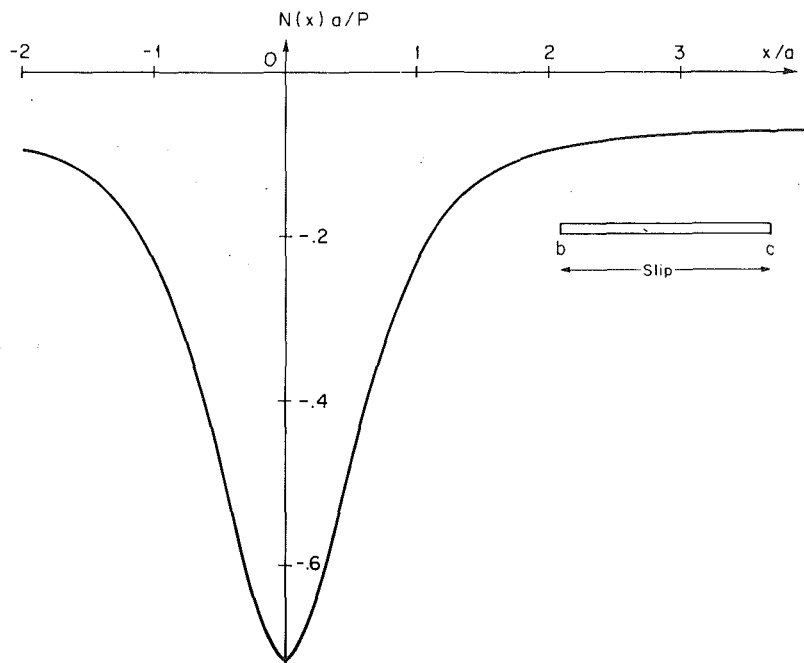


Fig. 6 Normal tractions for arrangement (b) with  $b/a = 1.5$ ,  $c/a = 2.3$ ,  $\lambda = 13.98$

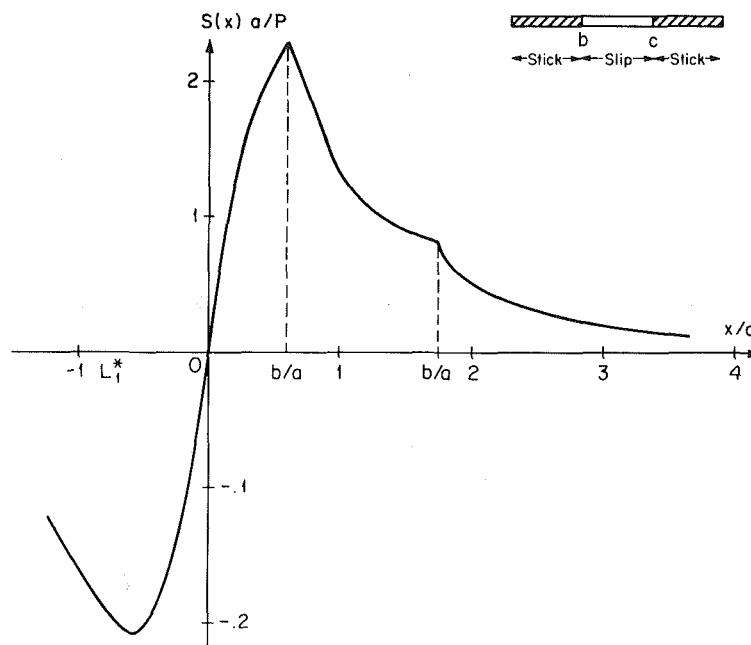


Fig. 7 Shear tractions for arrangement (c),  $b/a = 0.6$ ,  $c/a = 1.74$ ,  $\lambda = 8.22$

$B(x)$  is square root singular at the end points marking transition between slip and undamaged material and it is bounded at the transition between slip and stick. When  $B(x)$  is required to be bounded at both ends, as is the case for a detached slip zone, a consistency condition must be imposed on  $B(x)$ . This consistency condition is automatically included in the discretized system of equations obtained by the numerical method for singular integral equations of Erdogan et al. [10], which is employed here. For details of the application of the method to the present problem, the reader is referred to [1-3].

We note that for the arrangement of Fig. 2(a) there is only one unknown parameter,  $c$ . For Fig. 2(b), there are no

unknowns and for Fig 2(c) and 2(d)  $b$  and  $c$  are unknowns. For Fig. 2(e),  $b_1, b_2, c_2$  are unknowns and for Fig. 2(f)  $b_1$  and  $b_2$  are unknowns. In all arrangements, except that of Fig. 2(b), one of the unknowns can be replaced by the load parameter

$$\lambda = P/p_0 a \quad (18)$$

to simplify the numerical procedure. For instance, in the arrangement of Fig. 2(a),  $c$  was specified and  $\lambda$  was computed. In the arrangement of Fig. 2(c),  $b$  was specified and  $\lambda$  and  $c$  were computed, etc.

Results for the mirror image arrangements are not presented.

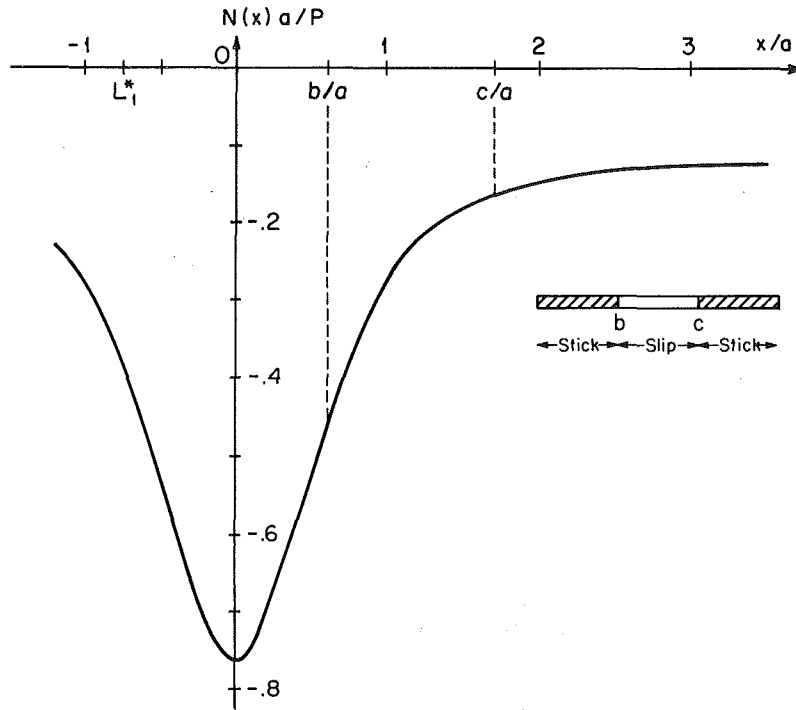


Fig. 8 Normal tractions for arrangement (c),  $b/a = 0.6$ ,  $c/a = 1.74$ ,  $\lambda = 8.22$

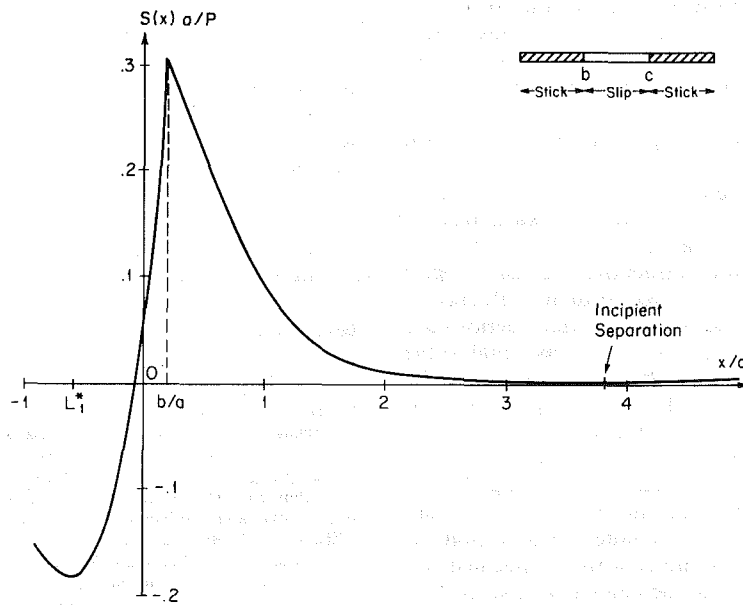


Fig. 9 Shear tractions for arrangement (c) at the onset of separation;  $b/a = 0.19$ ,  $c/a = 30.5$ ,  $\lambda = 563$

## Results

The results are summarized in Fig. 3 which gives the extent and the location of slip zones for a given value of the loading parameter  $\lambda$  and for  $f = 0.5$ . The two thick curves correspond to arrangement (d) and coincide with Fig. 6 of [1]. In this discussion, letter designations for slip arrangements correspond to those shown in Fig. 2.

Arrangement (a) is exemplified by a crack that starts at  $x = 1.5a$  ( $L_1 = b = 1.5a$ ). Slip starts at the crack tip  $L_1$  when  $P/p_0a = 8.3$  and extends to the right with increasing load. Eventually, the slip zone will extend to the right crack tip  $L_2$ , when transition to case (b) occurs. At this point, the shear stress intensity factor ahead of  $L_2$  is still zero, Fig. 4. If the

load is increased further, the shear tractions become singular ahead of  $L_2$ , Fig. 5. In both cases, the shear tractions are singular behind  $L_1$ . The corresponding normal tractions are practically the same as for the Flamant solution and are shown for one case in Fig. 6.

In arrangement (c) we start with one slip zone which is detached from the crack tips. The extent of the slip zone in this case differs only slightly from the right-hand zone in configuration (d) and the corresponding curve cannot be distinguished from the thick line in Fig. 3. With further increase of the load, slip reaches one of the crack tips leading to arrangement (a) or its mirror image. The case where the slip zone reaches the left tip first is illustrated in Fig. 3 for  $L_1 = b$

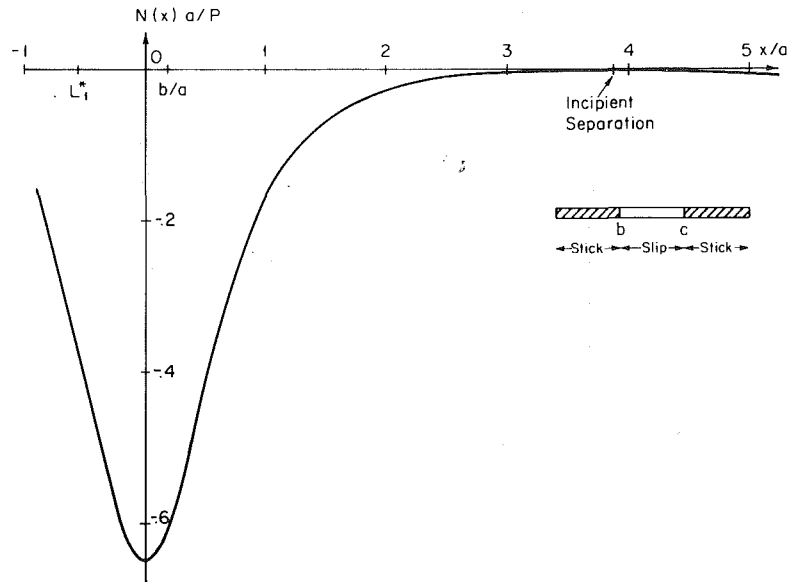


Fig. 10 Normal tractions for arrangement (c) at the onset of separation,  $b/a = 0.19$ ,  $c/a = 30.5$ ,  $\lambda = 563$

$= 0.75a$ . For this case, the right end of the slip zone  $c$  continues to follow curve (d) closely.

The configuration 2(e) must be preceded by (d) if  $L_1 < -a$  or by (c) if  $L_1 > -a$ . In the former case, the point  $b_1$  is very close to the left curve (d), while in the latter it falls inside this curve. In both cases, the curve for the right slip zone practically coincides with 2(d). Examples are shown with  $L_1 = -2a$  and  $L_1 = -0.9a$ .

Finally, an example for the arrangement (f) is shown with  $L_1 = -1.3a$  and  $L_2 = 0.9a$ .

The biggest deviations in the extent of the slip zones from curve (d) occur when the slip zone grows outward from a crack tip as in cases (a)<sub>1</sub>, (e)<sub>2</sub> of Fig. 3.

An example of shear and normal tractions is given in Fig. 7 and 8 for arrangement (c) and  $b = 0.6a$ . Note the influence of the slip zone on the shear tractions. The normal tractions are not much affected by slip and are approximately equal to the Flamant tractions. The location of the left crack tip can be arbitrary provided it does not extend beyond the point marked  $L_1^*$ , at which transition to arrangement (e) occurs.

When the load is very high in comparison with those shown in Fig. 3, the inequality (11) is violated, indicating the occurrence of separation, and the present analysis is not valid without modification. Here, we only note the conditions at the onset of separation. For example, with arrangement (c) separation starts approximately at the point  $x = 3.8a$  for  $\lambda = 563$  with  $b = 0.188a$  and  $c = 30.5a$ . The corresponding shear and normal tractions are shown in Fig. 9 and 10.

In arrangement (e) separation was observed for  $\lambda = 597$  in the vicinity of  $x = 3.8a$  corresponding to  $b_2 = 0.205a$ ,  $c_2 = 30.5a$ ,  $b_1 = -0.37a$  and  $c_1 = -2.2a$ . In arrangement (f) separation occurred for  $\lambda = 483$  at  $x \sim 3.7a$  and for symmetric slip zones  $b_2 = -b_1 = 0.265a$ ,  $c_2 = -c_1 = 23a$ . In arrangement (d) separation also starts for approximately the same parameters.

In arrangement (b) the load at which separation starts depends on the location and crack extent. For example, for  $b = 0.4a$  and  $c = 3a$  separation starts at  $x = 0.298a$  with  $\lambda =$

222, while for  $b = a$  and  $c = 5a$  separation starts at  $x = 4.39a$  with  $\lambda = 235$ .

The case of  $p_0 = 0$  corresponds to  $\lambda = \infty$ . It cannot be examined with the present formulation because of the presence of separation. For arrangement (d), which is equivalent to a layer resting on a substrate, the slip zones become very large in the limit  $\lambda = \infty$  and an increasing number of collocation points is required for convergence. For these reasons, the case of zero precompression is not examined here, but it will be considered in the future.

### Acknowledgment

Support by the Office of Naval Research through contract N00014-81-K-0626 is gratefully acknowledged.

### References

- 1 Comninou, M., Schmueser, D., and Dundurs, J., "Frictional Slip Between a Layer and Substrate Caused by a Normal Load," *International Journal of Engineering Science*, Vol. 18, 1980, pp. 131-137.
- 2 Schmueser, D., Comninou, M., and Dundurs, J., "Separation and Slip Between a Layer and a Substrate Caused by a Tensile Load," *International Journal of Engineering Science*, Vol. 18, 1980, pp. 1149-1155.
- 3 Schmueser, D., Comninou, M., and Dundurs, J., "Frictional Slip Between a Layer and a Substrate," *Journal of Engineering Mechanics Division, ASCE*, Vol. 107, 1981, pp. 1103-1118.
- 4 Comninou, M., Barber, J. R., and Dundurs, J., "Interface Slip Caused by a Surface Load Moving at Constant Speed," *International Journal of Mechanical Sciences*, Vol. 45, 1983, pp. 41-46.
- 5 Chang, F.-K., Comninou, M., and Barber, J. R., "Slip Between a Layer and a Substrate Caused by a Normal Force Moving Steadily Over the Surface," *International Journal of Mechanical Sciences*, in press.
- 6 Anscombe, H., and Johnson, K. L., "Slip of a Thin Solid Tyre Press-Fitted on a Wheel," *International Journal of Mechanical Sciences*, Vol. 16, 1972, pp. 525-534.
- 7 Hundy, B. B., "Shelling of Railway Wheels," *Railway Steel Topics*, Vol. 4, 1957, pp. 19-35.
- 8 Timoshenko, S. P., and Goodier, J. N., *Theory of Elasticity*, McGraw-Hill, New York, 1970.
- 9 Dundurs, J., and Comninou, M., "Some Consequences of the Inequality Conditions in Contact and Crack Problems," *Journal of Elasticity*, Vol. 9, 1979, pp. 71-82.
- 10 Erdogan, F., Gupta, G. D., and Cook, T. S., in *Methods of Analyses and Solution of Crack Problems*, Noordhoff, Leyden, 1973.